

# UC Irvine

## UC Irvine Previously Published Works

### Title

Frequent Low-Dose  $\Delta^9$ -Tetrahydrocannabinol in Adolescence Disrupts Microglia Homeostasis and Disables Responses to Microbial Infection and Social Stress in Young Adulthood

### Permalink

<https://escholarship.org/uc/item/2vr329rz>

### Journal

Biological Psychiatry, 92(11)

### ISSN

0006-3223

### Authors

Lee, Hye-Lim  
Jung, Kwang-Mook  
Fotio, Yannick  
et al.

### Publication Date

2022-12-01

### DOI

10.1016/j.biopsych.2022.04.017

Peer reviewed



Published in final edited form as:

*Biol Psychiatry*. 2022 December 01; 92(11): 845–860. doi:10.1016/j.biopsych.2022.04.017.

## Frequent low-dose $\Delta^9$ -tetrahydrocannabinol in adolescence disrupts microglia homeostasis and disables responses to microbial infection and social stress in young adulthood

Hye-Lim Lee<sup>1</sup>, Kwang-Mook Jung<sup>1</sup>, Yannick Fotio<sup>1</sup>, Erica Squire<sup>1</sup>, Francesca Palese<sup>1</sup>, Lin Lin<sup>1</sup>, Alexa Torrens<sup>1</sup>, Faizy Ahmed<sup>1</sup>, Alex Mabou Tagne<sup>1</sup>, Jade Ramirez<sup>1</sup>, Shiqi Su<sup>1</sup>, Christina Renee Wong<sup>1</sup>, Daniel Hojin Jung<sup>1</sup>, Vanessa M. Scarfone<sup>2</sup>, Pauline U. Nguyen<sup>2</sup>, Marcelo Wood<sup>3</sup>, Kim Green<sup>3</sup>, Daniele Piomelli<sup>1,4,5</sup>

<sup>1</sup>Department of Anatomy and Neurobiology, University of California, Irvine, USA.

<sup>2</sup>Sue and Bill Gross Stem Cell Research Center, University of California, Irvine, USA.

<sup>3</sup>Department of Neurobiology and Behavior, University of California, Irvine, USA.

<sup>4</sup>Department of Biological Chemistry, University of California, Irvine, USA

<sup>5</sup>Department of Pharmaceutical Sciences, University of California, Irvine, USA

### Abstract

**Background:** During adolescence, microglia are actively involved in neocortical maturation while concomitantly undergoing profound phenotypic changes. As teenage years are also a time of experimentation with cannabis, we evaluated whether adolescence exposure to the drug's psychotropic constituent,  $\Delta^9$ -tetrahydrocannabinol (THC), might persistently alter microglia function.

**Methods:** We administered THC (5 mg/kg, intraperitoneal) once daily to male and female mice from postnatal day (PND) 30 to PND44 and examined the transcriptome of purified microglia in adult animals (PND70 and PND120) under baseline conditions or following either of two interventions known to recruit microglia: lipopolysaccharide (LPS) injection and repeated social defeat (RSD). We used high-dimensional mass cytometry by time of flight to map brain immune cell populations after LPS challenge.

**Results:** Adolescence THC exposure produced in mice of both sexes a state of microglial dyshomeostasis which persisted until young adulthood (PND70) but receded with further aging (PND120). Key features of this state included broad alterations in genes involved in microglia homeostasis and innate immunity along with marked impairments in the responses to LPS and RSD-induced psychosocial stress. The endocannabinoid system was also dysfunctional. The effects of THC were prevented by coadministration of either a global CB<sub>1</sub> receptor inverse agonist or a peripheral CB<sub>1</sub> neutral antagonist and were not replicated when THC was administered in young adulthood (PND70–84).

---

Disclosures

The authors declare no competing interest.

**Conclusions:** Daily low-intensity CB<sub>1</sub> receptor activation by THC during adolescence may disable critical functions served by microglia until young adulthood with potentially wide-ranging consequences for brain and mental health.

### Keywords

<sup>9</sup>-Tetrahydrocannabinol; Adolescence; Microglia; Immune response; Social stress; Endocannabinoid

---

### Introduction

The use of cannabis is common in adolescence (1), a time when neocortical networks that underpin cognition are still developing (2) and may thus be especially vulnerable to the effects of cannabis' intoxicating constituent. <sup>9</sup>-tetrahydrocannabinol (THC) (3,4). Epidemiological surveys suggest that exposure to cannabis during the teenage years may be associated with impairments in cognition and affect that continue into adulthood even after use of the drug has stopped (5,6). Increased risk of developing schizophrenia has also been documented (7,8). Some of these findings have been questioned (see, for example, ref. 9) but, supporting their relevance, laboratory studies in rodents indicate that adolescent treatment with THC may cause lasting dysregulations in memory, emotion and reward-seeking behavior (10,11).

THC exerts its pharmacological effects by interacting with CB<sub>1</sub> and CB<sub>2</sub> cannabinoid receptors, two core components of the endocannabinoid system (12). This signaling complex – which also comprises lipid-derived ligands [anandamide and 2-arachidonoyl-*sn*-glycerol (2-AG)] and proteins involved in their formation and deactivation – regulates neuronal migration, axonal guidance, and synaptogenesis during prenatal and postnatal brain development (13). Moreover, in adolescence and adulthood, the endocannabinoid system constitutes the molecular scaffold for a retrograde signaling process that modulates synaptic plasticity throughout the central nervous system (CNS) (14,15). Like other neurotransmitters, the endocannabinoids undergo profound adaptations during adolescence. Experiments in rodents have shown that anandamide mobilization and CB<sub>1</sub> receptor expression in the brain reach their peak around mid-adolescence and decrease in adulthood (16–18). This transient upregulation may reflect the role played by endocannabinoid signals in two defining features of adolescent behavior – heightened sensitivity to natural and drug rewards, and increased propensity to seek novelty and take risks (19).

Endocannabinoid signals play important regulatory roles in microglia (20,21), specialized macrophages of CNS parenchyma that are critically involved in the maintenance of adult brain homeostasis (22,23). Microglia are long-lived, heterogenous in structure and function, and exquisitely responsive to developmental and environmental cues (24). Moreover, perturbations in their homeostasis have been implicated in the pathogenesis of neurodegenerative and psychiatric disorders (25–28). Of note, studies have shown that a variety of habit-forming substances – including psychostimulants and opioids – share the ability to disrupt microglial homeostasis (28). For example, in adult mice and rats, the emergence of tolerance to the antinociceptive effects of morphine is accompanied by

microglia activation in spinal cord (29,30). Long-lasting effects of habit-forming drugs on microglia have also been reported. In one landmark study, repeated morphine administration to adolescent male rats caused a regionally selective increase in the microglial expression of toll-like receptor 4 (TLR4), a marker of enhanced responsiveness to proinflammatory stimuli, which persisted until adulthood (31). This and other findings (28) suggest that exposure to certain pharmacological agents during adolescence might persistently affect microglia and, by doing so, alter physiological processes that depend on these cells. Here, we asked whether THC might be one such agent. Using a protocol designed and validated to mimic daily low-dose cannabis use, we found that THC administration in adolescent male and female mice – but not adult male mice – causes an enduring downregulation in the expression of microglial homeostatic and host-defense genes. This effect is prevented by global or peripheral CB<sub>1</sub> receptor blockade and is associated with a profound inability to mount appropriate responses to bacterial infection and psychosocial stress, two primary functions served by microglia in the adult brain (32,33).

## Methods and Materials

### Animals

Male and female C57BL/6 mice were purchased from Jackson Labs (Farmington, CT) and arrived at our facility on post-natal day (PND) 22–23. 12-month-old male CD-1 mice were obtained from Charles River (Wilmington, MS). All animals were housed in ventilated cages (4 per cage) with free access to chow and water in rooms maintained on a 12-h light/12-h dark cycle (lights on at 6:30 AM, off at 6:30 PM) with constant temperature (22±2°C) and humidity (55–60%). In female mice, estrous cycle was monitored daily with vaginal smears for at least one week before the experiments and only animals at the metestrus phase were used (34,35). All procedures were approved by the Institutional Animal Care and Use Committee of the University of California, Irvine, and were carried out in strict accordance with the National Institutes of Health guidelines for care and use of experimental animals.

### Cell Isolation

We digested mouse brain tissue using a commercial kit (Miltenyi Biotec, Bergisch Gladbach, Germany). Dissociated cells were incubated with anti-CD11b, anti-CD11a and anti-CD45 antibodies in an antibody-staining buffer containing 0.2% (w/v) bovine serum albumin and 0.1% (w/v) sodium azide in phosphate-buffered saline (Supplemental Table 1) for 30 min at 4°C. Microglia were isolated by Fluorescence-Activated Cell Sorting (FACS), as illustrated in Supplemental Fig. S1A. Cell type markers used for FACS gating are listed in Supplemental Table 2. Debris, cell doublets, and dead cells were removed through cell gating, and microglia were isolated by selecting CD45<sup>+</sup>/CD11b<sup>+</sup>/CD11a<sup>lo</sup> cells (Supplemental Fig. S1B). Infiltrating CD11a<sup>hi</sup> macrophages were separated from CD11a<sup>lo</sup> microglia (Supplemental Fig. S1B). Enrichment in microglia was verified by comparing the absolute values of reads per kilobase of exon per million reads mapped (FPKM) for all quantifiable RNAs (Supplemental Fig. S1C). To circulating immune cells, blood was collected by cardiac puncture and erythrocytes were removed using a commercial buffer (Miltenyi Biotec). Remaining cells were incubated with anti-Ly6C and anti-Ly6G antibodies in antibody-staining buffer for 30 min at 4°C (Supplemental Tables 1 and 2). Ly6C<sup>+</sup> and

Ly6G<sup>+</sup> cells were considered inflammatory monocytes. FACS-sorted cells were quantified using FCS Express 7 (De Novo Software, Pasadena, CA).

## Other Methods

All other Methods and Materials, including Statistical Analyses, are reported in the Supplemental Methods section.

## Results

### A model of frequent low-dose THC exposure in adolescence

To approximate frequent low-dose cannabis use in adolescence we administered THC (5 mg/kg, i.p.) or its vehicle to mice once daily from PND30 to PND43 (Fig. 1A), an interval that spans adolescence in laboratory rodents (36). At this dosage, the drug achieved a peak plasma concentration ( $C_{max}$ ) of  $331 \pm 66$  ng/ml ( $1.11 \pm 0.17$  nmol/ml,  $n = 4$ ) at a time to maximum ( $T_{max}$ ) of 15 min and exhibited a half-life time of elimination ( $t_{1/2}$ ) of  $75 \pm 9$  min (Fig. 1B). This exposure level produces modest effects in adolescent male mice (37) and, in the present experiments, resulted in a small decrease in body temperature (THC:  $-1.04 \pm 0.1^\circ\text{C}$ ; vehicle:  $0.23 \pm 0.1^\circ\text{C}$ ;  $n = 5$ ) which was not accompanied by any change in food intake or motor activity (Fig. 1B). We stopped treatment at PND43 and assessed microglial gene expression at PND49 (when THC was no longer detectable in brain but was still present in fat) (Fig. 1C), PND70 (when THC was cleared from the body) and PND120.

### Adolescence THC exposure causes persistent transcriptional alterations in microglia

We isolated microglia from THC- and vehicle-treated mice and profiled their transcriptome by bulk RNA sequencing at PND49 and PND70 (Supplemental Fig. S1). The four datasets were readily distinguishable by principal component analysis, with both age and treatment contributing to variance (Fig. 2A). The total number of genes differentially expressed between control and THC-treated animals was 3976 at PND49 and 2359 at PND70 (Fig. 2B, Supplemental Table 3). Gene ontology (GO) annotation revealed a substantial downregulation of host-defense pathways (Fig. 2C). Categories most affected at PND70 included endocytosis (GO:0006897), response to bacterial molecules (GO:0002237), positive regulation of immune response (GO:0050778 and GO:0045087), response to lipopolysaccharide (LPS) (GO:0032496), and immune-activating signal transduction (GO:0002757). Closer inspection of the data showed that transcription of multiple genes involved in innate immunity – e.g., those encoding interleukin  $1\beta$  (*Il1b*), interleukin 6 (*Il6*), retinoic acid receptor- $\alpha$  (*Rara*), cyclooxygenase-2 (*Ptgs2*), cluster of differentiation 74 (*Cd74*) and several members of the Toll-like receptor family (*Tlr2*, *Tlr3*, *Tlr7*, *Tlr9*) – was attenuated at both PND49 and PND70 (Fig. 2D). Notably, expression of cluster of differentiation 36 (*Cd36*) rose  $\sim 22.6$  folds at PND49 to decline below control levels at PND70 (Fig. 2D). Genes that are critical to the control of microglia homeostasis – e.g., transforming growth factor- $\beta 1$  (*Tgfb1*) and its two receptors (*Tgfb1* and *Tgfb2*), MAF BZIP transcription factor B (*Matb*) and early growth response 1 (*Egr1*) – were also variously affected (Fig. 2E), while genes that are upregulated in disease-associated microglia (38) were either unchanged (e.g., *Axl*, *Spi1* and *Trem2*) or attenuated [e.g., *ApoE* and *Clec7a* (dectin-1)] at PND49 and/or PND70 (Fig. 2F). A notable exception

was microRNA-155 (*miR-155hg*), whose transcription was persistently elevated in the THC group (Fig. 2F). Consistent with lasting modifications in microglial homeostasis, immunofluorescent imaging experiments revealed that levels of ionized calcium binding adaptor molecule 1 (IBA-1) (39) were lower in hippocampus of male THC-exposed mice at both PND49 and PND70, compared to controls (Fig. 2G and 2H). Morphometric analyses further showed that the maximal length of microglial processes was greater in THC-treated male mice than controls (Fig. 2I). The number of ramified IBA-1-positive cells was modestly, and insignificantly, higher in THC-exposed animals (Fig. 2I) whereas other parameters, including number of IBA-1-positive cells, remained unchanged (Supplemental Fig. S2). qRT-PCR quantification of representative THC-sensitive mRNAs indicated that microglia transcription in the THC group returned to normal by PND120 (Fig. 2J). Further interrogation of the data using the STRING platform (<https://string-db.org>) showed that microglia from THC-exposed animals exhibited significant changes in sense-related transcripts (40) and, more specifically, in the *Tyrobp* causal network that is critically involved in innate immunity (Fig. 3) (41). The results indicate that daily exposure to low-dose THC during adolescence causes substantial modifications in the microglial transcriptome, which persist until young adulthood.

### Adolescence THC exposure alters endocannabinoid signaling in microglia

Cannabinoid receptor overactivation during adolescence may cause enduring modifications in endocannabinoid signaling (3). Accordingly, RNA sequencing of purified microglia at PND49 identified multiple alterations in genes encoding for components of the endocannabinoid system, some of which persisted until PND70 (Fig. 4A and 4B). Such alterations, which were confirmed by qRT-PCR, included transient and opposite changes in CB<sub>1</sub> (*Cnr1*) and CB<sub>2</sub> (*Cnr2*) receptors (Fig. 4C), a persistent increase in fatty acid amide hydrolase (*Faah*) (Fig. 4D) along with concomitant decreases in *N*-acyl phosphatidylethanolamine-selective phospholipase D (*Napepld*) and monoglyceride lipase (*Mgl1*) (Fig. 4E and 4F). The transcription of *N*-acylethanolamine acid amidase (*Naaa*), a cysteine hydrolase that degrades the paracannabinoid lipid palmitoylethanolamide (12,42), was also persistently reduced (Fig. 4G). Levels of the aforementioned transcripts returned to normal by PND120 (Fig. 4C–G).

### Adolescence THC exposure disables the response to bacterial endotoxin

Microglia are the first line of defense against microbial agents invading the brain (32). To determine whether this function might be affected by adolescence THC exposure, we challenged control and THC-treated male mice with LPS (0.33 mg/kg, i.p.). The bacterial endotoxin was administered on PND70, and brains were collected 24h later for RNA sequencing. We analyzed both whole brain extracts, to evaluate the organ's defense response in its entirety, and FACS-purified microglia. Compared to saline, LPS produced broad transcriptional changes in brain of animals not exposed to THC: a total of 268 genes were differentially expressed (Fig. 5A), with largest increases observed in immune pathways – e.g., interferon regulatory factor 7 (*Irf7*), interferon induced transmembrane protein 3 (*Ifitm3*), complement component C4b (*C4b*),  $\beta_2$ -microglobulin (*B2m*) and lymphocyte activation protein-6A (*Ly6a*) (Fig. 5B; Supplemental Table 4). The three GO categories most significantly upregulated following LPS challenge were immune process (GO:0002376),

defense response (GO:0006952) and response to external biotic stimuli (GO:0043207) (Fig. 5C). As expected, LPS also enhanced transcription of representative cytokines – interleukin 1 $\beta$  (*Il1b*), interleukin 6 (*Il6*) and tumor necrosis factor- $\alpha$  (*Tnfa*) – in purified microglia (Supplemental Fig. S3).

The effect of LPS was blunted in THC-exposed mice (Fig. 5A and 5B, Supplemental Fig. S3), in which the most enriched GO categories were not related to immunity (Fig. 5D). Only 47 differentially expressed genes, primarily involved in host defense, were shared between THC-treated and control mice following LPS challenge (Fig. 5E): these comprised response to biotic stimuli (GO:0043207, GO:0009607), response to other organisms (GO:0051707, GO:0098542) and immune response (GO:0006955). Confirming these findings, qRT-PCR and ELISA analyses of brain extracts showed that expression of *Il1b*, *Il6* and *Tnfa* was attenuated in THC-exposed animals, compared to controls, both 6h and 24h after LPS injection (Fig. 5F; protein levels are shown in Supplemental Fig. S4). Adolescence THC treatment also reduced the rise in hippocampal IBA-1 (Fig. 5G, 5H) and the number of monocytes found in bloodstream and brain 24h after LPS administration (Fig. 6). The endotoxin's proinflammatory effect was restored at PND120 (Supplemental Fig. S5).

High-dimensional mass cytometry by time-of-flight (cyTOF) (43) offered additional insights into the impact of adolescence THC exposure on immune cell populations of the brain. We purified CD45-positive cells from brains of PND70 mice treated with LPS or vehicle and analyzed them by cyTOF using a panel of 25 heavy metal isotope-tagged antibodies (Supplemental Table 5) (Fig. 7A). Consistent with previous reports (44), stochastic neighbor embedding (viSNE) analysis of the data (45) identified four cell populations: microglia, dendritic cells, border-associated macrophages, and monocytes (Fig. 7B1, Supplemental Fig. S6). Microglia were further divided into two subpopulations: surveillant, which was predominant in mice not treated with LPS (Fig. 7B2), and activated, which became prevalent after LPS administration (Fig. 7B3). LPS also increased the number of monocytes in the brain (Fig. 7B2 and 7B3). Adolescence THC treatment did not grossly alter this profile (Fig. 7B4). However, viSNE interrogation of cell-marker densities (Fig. 7C) suggested multiple dissimilarities between THC-treated and control mice (Fig. 7C3 and 7C4), which could be resolved using spanning-tree progression analysis of density-normalized events (SPADE) (46). This tool identified five microglial clusters that differed between THC and control groups (Fig. 7D). Distinguishing features shared among these clusters included lower expression of proinflammatory proteins (interleukin 17A, CD68, and MHCII) and higher expression of FAAH and CD81, an extracellular vesicle marker (47) (Fig. 7E). Higher levels of the T-cell costimulatory molecule CD86 (48) were found in clusters 1 and 2, while higher levels of F4/80, which might play a role in antigen recognition (49), were seen in clusters 1 and 4 (Fig. 7E). Together, the findings indicate that adolescence THC exposure causes a persistent disruption in the molecular and cellular response of microglia to gram-negative bacterial infection.

### Adolescence THC exposure impairs the response to psychosocial stress

Microglial activation mediates the response to social stress in rodent models (33) and has been linked to the development of depression in humans (27,50). The finding that



adolescence THC treatment causes an enduring impairment in microglia-mediated host defense prompted us to ask whether reactions to psychosocial stress might also be affected. To test this, we subjected young-adult male mice (PND70) that had received either THC or vehicle during adolescence to a repeated social defeat (RSD) protocol (Fig. 8A and 8B). This paradigm reproduces key aspects of the human response to social stress and is known to depend on microglial activation (51–53). Predictably, in vehicle-treated animals RSD produced marked elevations in circulating corticosterone and IL-6 concentrations (Fig. 8C and 8D) and stimulated transcription of *I1b*, *I16* and *Tnfa* in brain (Fig. 8E). Strikingly, no such effect occurred in THC-treated animals (Fig. 8C–E).

Next, we assessed the impact of RSD on social anxiety using the social interaction test (51,54,55). In control mice, RSD caused social withdrawal, as shown by an increase in time spent in the avoidance zone of the arena (Fig. 8F) and a reduction in time spent in the social interaction zone (Fig. 8G). As reported (51,56), ~75% of defeated mice in the control group showed an impairment in social behavior while the remainder were resilient (Fig. 8G). By contrast, none of the animals in the THC group developed social withdrawal after RSD (Fig. 8F and 8G), a difference that cannot be ascribed to variability in aggression time (Fig. 8H). Finally, we evaluated innate fear using the elevated plus maze test under non-aversive conditions. As anticipated (54), RSD produced robust anxiety-like behavior in vehicle-treated mice, evidenced by a decrease in the time spent in, and the number of entries into, the open arms of the maze (Fig. 8I and 8J, Supplemental Fig. S7). Conversely, animals in the THC group exhibited no overt change in anxiety-like behavior (Fig. 8I and 8J, Supplemental Fig. S7). We conclude that the response to psychosocial stress is defective in young-adult male mice exposed to THC during adolescence.

### Role of CB<sub>1</sub> cannabinoid receptors

The psychoactive effects of THC depend on activation of CB<sub>1</sub> receptors, which are highly expressed in CNS but are also found throughout the periphery (57,58). We asked therefore whether CB<sub>1</sub> blockade might prevent the temporary disruption in microglia homeostasis caused by adolescent THC (Fig. 9A). Coadministration of THC with the global CB<sub>1</sub> inverse agonist AM251 (1 mg/kg, i.p., once daily 30 min before THC) prevented changes in transcription of representative THC-sensitive genes in purified microglia both under control conditions and after LPS stimulation (Fig. 9B–D). Interestingly, coadministration of THC and AM6545 (3 mg/kg, i.p.), a CB<sub>1</sub> neutral antagonist that does not access the CNS (59), produced a similar effect (Fig. 9B–D). We interpret the results as indicating that adolescence THC exposure temporarily affects microglia homeostasis through a mechanism that requires the engagement of CB<sub>1</sub>-expressing cells outside the CNS.

### Effects of sex and age

Since sex influences microglial gene expression (60,61) and function (62,63), we examined whether female mice might be sensitive to the long-term consequences of adolescence THC exposure (Fig. 10A), as seen with males. Baseline and LPS-stimulated expression of representative cytokines was suppressed in purified microglia from young-adult female mice that had received THC during adolescence (Fig. 10B–D; brain mRNA levels are shown in Supplemental Fig. S8). Moreover, (i) no significant sex differences were observed in the



response of endocannabinoid-related genes in either purified microglia or brain extracts, whereas (ii) a sexual dimorphism transpired in Iba-1 expression and morphometric microglia measurements, with female mice failing to display the phenotypic changes observed in males (Supplemental Fig. S8). Confirming previous work (64), sex-related differences in the quantitative response to LPS were also noted (Fig. 10B–D).

Microglial properties change during postnatal development (24). We asked therefore whether microglia in young-adult male mice might be vulnerable to the persistent effects of repeated THC exposure, as shown for adolescent male and female mice. We injected THC (5 mg/kg, i.p.) once daily for 14 days starting on PND70 and sacrificed the mice 27 days later (PND110) (Fig. 10E). The volcano plot reported in Figure 10F shows that only 22 genes were differentially expressed between control and THC groups, none of which is involved in immunity (Supplemental Table 6). Furthermore, all genes whose expression was changed by adolescent THC remained unaltered when the same treatment was given in adulthood (Fig. 10G).

## Discussion

The results show that daily exposure to low-dose THC produces in adolescent male and female mice a persistent disruption of microglia transcription and function, which lasts until young adulthood (PND70) and recedes when the animals transition to full maturity (PND120). This state is prevented by either global or peripheral CB<sub>1</sub> receptor blockade and is characterized by (i) changes in the expression of genes that underpin microglial homeostasis and innate immunity; and (ii) impairments in microglia-driven responses to endotoxin challenge and psychosocial stress. The results suggest that frequent low-intensity activation of CB<sub>1</sub> receptors during adolescence disables critical functions served by microglia until young adulthood, with potentially far-reaching consequences for brain health.

We adopted an administration regimen that consisted of daily intraperitoneal injections of 5 mg/kg THC throughout adolescence, which in mice spans the fifth and sixth weeks of postnatal life (36). After a single injection, the plasma C<sub>max</sub> value for THC was comparable to those measured in blood of adult human smokers of ‘low-potency’ cannabis (~3% THC) experiencing signs of intoxication (65,66). In agreement with pharmacokinetic data and previous work (37), we found that this THC dosage elicited only modest effects in adolescent male mice (Fig. 1B) suggesting that the present protocol offers an ecologically relevant model for frequent low-intensity THC exposure. It is important to point out that this protocol was not designed to capture high-intensity use patterns – such as multiple daily usage of concentrated cannabis extracts – whose effects might be different from those described here. Indeed, prior work showed that high-intensity THC regimens (e.g., twice-daily injections escalating from 2.5 to 10 mg/kg over 10 days) in adolescent rats produce signs of neuroinflammation when animals reach adulthood (67–71).

Adolescence THC exposure modified the transcriptional profile of adult microglia in various ways. First, expression of many genes involved in innate immunity was attenuated. For example, genes encoding interleukin 1 $\beta$ , interleukin 6, cyclooxygenase-2, and various

members of the Toll-like receptor family were downregulated in microglia of THC-treated mice relative to controls (Fig. 2D). Indeed, data annotation using the STRING functional enrichment analysis suggested marked changes in the microglia sensome (40) as well as disruption of the *Tyrobp/Dap12* signaling pathway (Fig. 3A, B), whose roles in microglia activation are well documented (72). Second, multiple genes that contribute to microglia homeostasis – e.g., *Tgfb1*, *Tgfb1*, *Tgfb2*, *Mafb*, *Egr1* (26) – were variously altered (Fig. 2E) while genes that are upregulated in disease-associated microglia (24,26) either remained unchanged (*Axl*, *Spi1* and *Trem2*) or were downregulated (*Apoe*, *Clec7a*, *Itgax*) (Fig. 2F). Lastly, IBA-1 immunoreactivity was lower and maximal branch length of IBA-1-positive cells was higher in THC-exposed male mice compared to controls (Fig. 2G and 2H) though, as discussed below, this effect was not observed in females. Differences between vehicle and THC groups were brought into sharper focus after LPS challenge, whose impact on the expression of host-defense genes and monocyte trafficking was dampened in THC-treated mice (Figs. 5 and 6). A plausible interpretation of these results is that frequent exposure to THC in adolescence promotes an activation-resistant microglial phenotype that lasts until young adulthood. This scenario is consistent with the known immunosuppressive properties of THC (73) but should not be oversimplified. Indeed, its complexity is underscored by the enhanced transcription of microRNA-155 (Fig. 2F), whose pro-inflammatory functions are well recognized (74,75).

Another striking consequence of adolescence THC exposure was the suppression of molecular and behavioral responses to psychosocial stress, as assessed using the RSD model. In this paradigm, the stress caused by social defeat in repeated resident-intruder encounters produces a depression-like phenotype in which anxiety and social avoidance are accompanied by accelerated egress of monocytes from bone marrow and their recruitment to the brain (76). Based on our transcriptomic data, we expected that the response to RSD would be defective but were surprised by the size of the deficit we found. None of the hormonal and immune reactions that define this model – including increased circulating corticosterone and interleukin-6, and elevated inflammatory cytokine transcription in brain – was detectable in THC-exposed mice (Fig. 8C–E). Alterations in social and anxiety-like behaviors were also absent (Fig. 8F–J). The findings indicate that adolescence THC exposure causes a lasting inability to mount an adequate reaction to psychosocial stress. Since the processing of acute stress events in early life is essential to establish neuroimmune homeostasis (77,78), the potential mental health implications of this deficit warrant further examination.

THC's ability to persistently modify microglia was restricted to adolescence (Fig. 10F and 10G). This suggests that THC exposure early in life – when these cells still retain part of the heterogeneity typical of their embryonic stage (24) – may promote the establishment of an activation-resistant phenotype that lasts until young adulthood (PND70) and dissipates when the animal reaches full maturity (PND120). This hypothesis is consistent with microglia's longevity (79) and highlights the need to elucidate the mechanisms underpinning THC's impact on postnatal microglia function. Adolescence THC treatment lowered the expression of proinflammatory cytokines in microglia purified from the brain of both male and female mice (Fig. 10B–D). There were detectable sex differences, however, including (*i*) a greater number of elongated microglia branches, which was observed in THC-treated males but not

females; and (ii) the size of the stimulatory effect of LPS on cytokine transcription, which was greater in females than males irrespective of prior THC exposure. Sexual dimorphisms in microglia gene expression profile and function have been previously documented (80).

The impact of adolescence THC treatment on microglia requires CB<sub>1</sub> receptor activation (Fig. 9). Despite its moderate intensity, such activation was sufficient to evoke broad adaptations in the expression of endocannabinoid-related genes not only at PND49, when residual THC was still detectable in fat, but also three weeks later, when the drug had been eliminated from the body. Two such adaptations are especially noteworthy. First, transcription of the anandamide-producing enzyme NAPE-PLD was *decreased* whereas transcription of the anandamide-degrading enzyme FAAH was *increased*. Second, transcription of the 2-AG-degrading enzyme MGL was suppressed. These changes, which were maximal at PND49 but still statistically detectable at PND70, are suggestive of opposing modifications in 2-AG- and anandamide-mediated signaling in microglia. It is possible that these modifications contribute to the induction and/or maintenance of the microglial phenotype – for example, by enhancing immunosuppressant 2-AG-mediated signaling at CB<sub>1</sub> (73).

Another important question raised by our experiments pertains to the cellular localization of the CB<sub>1</sub> receptors engaged by THC. We found that the drug's lasting effects could be prevented by coadministering the peripheral CB<sub>1</sub> antagonist AM6545. This finding was not entirely unexpected. In fact, emerging evidence points to the existence of a functional crosstalk between microglia and circulating monocytes, which has been implicated in the response to social stress (81) as well as in the emergence of chronic pain (82) and neuroinflammation (83). It is thus plausible, though remains to be demonstrated, that THC's impact on microglia might require CB<sub>1</sub> activation in monocytes (84, 85) or other myeloid cells which might, for example, interrupt chemical communication with microglia. Consistent with this view, THC treatment lowered the numbers of monocytes in circulation and trafficking to the brain following LPS challenge (Fig. 6).

In conclusion, adolescence exposure to low-dose THC may induce in mice of both sexes a persistent state of microglia dishomeostasis that is accompanied by profound deficits in the molecular, hormonal, cellular and behavioral response to endotoxin and psychosocial stress. The emergence of this phenotype requires recruitment of peripheral CB<sub>1</sub> receptors and is accompanied by alterations in endocannabinoid signaling in microglia. Integrating these findings into epidemiological and clinical studies on adolescent brain development may help identify neuroimmune risks of early-life cannabis exposure, which may have been hitherto underestimated.

## Supplementary Material

Refer to Web version on PubMed Central for supplementary material.

## Acknowledgments

This work was supported by the National Institutes on Drug Abuse (NIDA) center grant P50DA044118-01.

## References

1. Carliner H, Brown QL, Sarvet AL, Hasin DS (2017): Cannabis use, attitudes, and legal status in the U.S.: A review. *Prev Med* 104:13–23. [PubMed: 28705601]
2. Kolk SM, Rakic P (2021): Development of prefrontal cortex. *Neuropsychopharmacology* <https://doi:10.1038/s41386-021-01137-9>.
3. Rubino T, Parolaro D. (2008): Long lasting consequences of cannabis exposure in adolescence. *Mol Cell Endocrinol* 286(1–2 Suppl 1):S108–S113. [PubMed: 18358595]
4. Levine A, Clemenza K, Rynn M, Lieberman J (2017): Evidence for the risks and consequences of adolescent cannabis exposure. *J Am Acad Child Adolesc Psychiatry* 56:214–225. [PubMed: 28219487]
5. Albaugh MD, Ottino-Gonzalez J, Sidwell A, Lepage C, Juliano A, Owens MM, et al. (2021): Association of cannabis use during adolescence with neurodevelopment. *JAMA Psychiatry* 78:1031–1040.
6. Schweinsburg AD, Brown SA, Tapert SF (2008): The influence of marijuana use on neurocognitive functioning in adolescents. *Curr Drug Abuse Rev* 1:99–111. [PubMed: 19630709]
7. Chadwick B, Miller ML, Hurd YL (2013): Cannabis use during adolescent development: susceptibility to psychiatric illness. *Front Psychiatry* 4:129. [PubMed: 24133461]
8. Renard J, Krebs MO, Le Pen G, Jay TM (2014): Long-term consequences of adolescent cannabinoid exposure in adult psychopathology. *Front Neurosci* 8:361. [PubMed: 25426017]
9. Rogeberg O (2013): Correlations between cannabis use and IQ change in the Dunedin cohort are consistent with confounding from socioeconomic status. *Proc Natl Acad Sci U S A* 110:4251–4254. [PubMed: 23319626]
10. Schneider M (2008): Puberty as a highly vulnerable developmental period for the consequences of cannabis exposure. *Addict Biol* 13:253–263. [PubMed: 18482434]
11. Rubino T, Parolaro D (2016): The impact of exposure to cannabinoids in adolescence: insights from animal models. *Biol Psychiatry* 79:578–585. [PubMed: 26344755]
12. Piomelli D, Mabou Tagne A (2021): Endocannabinoid-based therapies. *Annu Rev Pharmacol Toxicol* 62. [10.1146/annurev-pharmtox-052220-021800](https://doi.org/10.1146/annurev-pharmtox-052220-021800).
13. Harkany T, Cinquina V (2021): Physiological rules of endocannabinoid action during fetal and neonatal brain development. *Cannabis Cannabinoid Res* 6(5):381–388. [PubMed: 34619043]
14. Piomelli D (2014): More surprises lying ahead. The endocannabinoids keep us guessing. *Neuropharmacology* 76 Pt B:228–234. [PubMed: 23954677]
15. Piomelli D (2003): The molecular logic of endocannabinoid signalling. *Nat Rev Neurosci* 4:873–884. [PubMed: 14595399]
16. Laprairie RB, Kelly ME, Denovan-Wright EM (2012): The dynamic nature of type 1 cannabinoid receptor (CB1) gene transcription. *Br J Pharmacol* 167:1583–1595. [PubMed: 22924606]
17. Wenger T, Gerendai I, Fezza F, Gonzalez S, Bisogno T, Fernandez-Ruiz J, et al. (2002): The hypothalamic levels of the endocannabinoid, anandamide, peak immediately before the onset of puberty in female rats. *Life Sci*. 70:1407–1414. [PubMed: 11883716]
18. Casey BJ, Glatt CE, Lee FS (2015): Treating the developing versus developed brain: translating preclinical mouse and human studies. *Neuron* 86:1358–1368. [PubMed: 26087163]
19. Balogh KN, Mayes LC, Potenza MN (2013): Risk-taking and decision-making in youth: relationships to addiction vulnerability. *J Behav Addict* 2:10.1556/JBA.2.2013.1.1.
20. Stella N (2009): Endocannabinoid signaling in microglial cells. *Neuropharmacology* 56 Suppl 1(Suppl 1):244–253. [PubMed: 18722389]
21. Duffy SS, Hayes JP, Fiore NT, Moalem-Taylor G (2021): The cannabinoid system and microglia in health and disease. *Neuropharmacology* 190:108555. [PubMed: 33845074]
22. Ransohoff RM, Cardona AE (2010): The myeloid cells of the central nervous system parenchyma. *Nature* 468:253–262. [PubMed: 21068834]
23. Prinz M, Masuda T, Wheeler MA, Quintana FJ (2021): Microglia and central nervous system-associated macrophages – from origin to disease modulation. *Annu Rev Immunol* 39:251–277. [PubMed: 33556248]

24. Masuda T, Sankowski R, Staszewski O, Prinz M (2020): Microglia heterogeneity in the single-cell era. *Cell Rep* 30:1271–1281. [PubMed: 32023447]
25. Song WM, Colonna M (2018): The identity and function of microglia in neurodegeneration. *Nat Immunol* 19:1048–1058. [PubMed: 30250185]
26. Butovsky O, Weiner HL (2018): Microglial signatures and their role in health and disease. *Nat Rev Neurosci* 19:622–635. [PubMed: 30206328]
27. Mondelli V, Vernon AC, Turkheimer F, Dazzan P, Pariante CM (2017): Brain microglia in psychiatric disorders. *Lancet Psychiatry* 4:563–572. [PubMed: 28454915]
28. Catale C, Bussone S, Lo Iacono L, Carola V (2019): Microglial alterations induced by psychoactive drugs: A possible mechanism in substance use disorder?. *Semin Cell Dev Biol* 94:164–175. [PubMed: 31004753]
29. Leduc-Pessah H, Weilingner NL, Fan CY, Burma NE, Thompson RJ, Trang T (2017): Site-specific regulation of P2X7 receptor function in microglia gates morphine analgesic tolerance. *J Neurosci* 37:10154–10172. [PubMed: 28924009]
30. Qu J, Tao XY, Teng P, Zhang Y, Guo CL, Hu L, et al. (2017): Blocking ATP-sensitive potassium channel alleviates morphine tolerance by inhibiting HSP70-TLR4-NLRP3-mediated neuroinflammation. *J Neuroinflammation* 14:228. [PubMed: 29178967]
31. Schwarz JM, Bilbo SD (2013): Adolescent morphine exposure affects long-term microglial function and later-life relapse liability in a model of addiction. *J Neurosci* 33:961–971. [PubMed: 23325235]
32. Mariani MM, Kielian T (2009): Microglia in infectious diseases of the central nervous system. *J Neuroimmune Pharmacol* 4:448–461. [PubMed: 19728102]
33. Ramirez K, Fornaguera-Trías J, Sheridan JF (2017): Stress-induced microglia activation and monocyte trafficking to the brain underlie the development of anxiety and depression. *Curr Top Behav Neurosci* 31:155–172. [PubMed: 27352390]
34. Goldman JM, Murr AS, Cooper RL (2007): The rodent estrous cycle: characterization of vaginal cytology and its utility in toxicological studies. *Birth Defects Res B Dev Reprod Toxicol* 80:84–97. [PubMed: 17342777]
35. McLean AC, Valenzuela N, Fai S, Bennett SA (2012): Performing vaginal lavage, crystal violet staining, and vaginal cytological evaluation for mouse estrous cycle staging identification. *J Vis Exp* 67:e4389.
36. Dutta S, Sengupta P (2016): Men and mice: Relating their ages. *Life Sci* 152:244–248. [PubMed: 26596563]
37. Torrens A, Vozella V, Huff H, McNeil B, Ahmed F, Ghidini A, et al. (2020): Comparative pharmacokinetics of  $\Delta^9$ -tetrahydrocannabinol in adolescent and adult male mice. *J Pharmacol Exp Ther* 374:151–160. [PubMed: 32345621]
38. Deczkowska A, Keren-Shaul H, Weiner A, Colonna M, Schwartz M, Amit I (2018): Disease-associated microglia: A universal immune sensor of neurodegeneration. *Cell* 173:1073–1081. [PubMed: 29775591]
39. Imai Y, Kohsaka S (2002): Intracellular signaling in M-CSF-induced microglia activation: role of Iba1. *Glia* 40:164–174. [PubMed: 12379904]
40. Hickman SE, Kingery ND, Ohsumi TK, Borowsky ML, Wang LC, Means TK, et al. (2013): The microglial sensome revealed by direct RNA sequencing. *Nat Neurosci*. 16(12):1896–905. [PubMed: 24162652]
41. Zhang B, Gaiteri C, Bodea LG, Wang Z, McElwee J, Podtelezchnikov AA, et al. (2013): Integrated systems approach identifies genetic nodes and networks in late-onset Alzheimer’s disease. *Cell*. 153(3):707–20. [PubMed: 23622250]
42. Piomelli D, Scalvini L, Fotio Y, Lodola A, Spadoni G, Tarzia G, et al. (2020): N-Acylethanolamine Acid Amidase (NAAA): Structure, function, and inhibition. *J Med Chem* 63:7475–7490. [PubMed: 32191459]
43. Bandura DR, Baranov VI, Ornatsky OI, Antonov A, Kinach R, Lou X, et al. (2009) Mass cytometry: technique for real time single cell multitarget immunoassay based on inductively coupled plasma time-of-flight mass spectrometry. *Anal Chem*. 81(16):6813–22. [PubMed: 19601617]

44. Mrdjen D, Pavlovic A, Hartmann FJ, Schreiner B, Utz SG, Leung BP, et al. (2018): High-Dimensional Single-Cell Mapping of Central Nervous System Immune Cells Reveals Distinct Myeloid Subsets in Health, Aging, and Disease. *Immunity*. 48(2):380–395.e6. [PubMed: 29426702]
45. Amir el-AD, Davis KL, Tadmor MD, Simonds EF, Levine JH, Bendall SC, et al. (2013): viSNE enables visualization of high dimensional single-cell data and reveals phenotypic heterogeneity of leukemia. *Nat Biotechnol*. 31(6):545–52. [PubMed: 23685480]
46. Qiu P, Simonds EF, Bendall SC, Gibbs KD Jr, Bruggner RV, Linderman MD, et al. (2011): Extracting a cellular hierarchy from high-dimensional cytometry data with SPADE. *Nat Biotechnol*. 29(10):886–91. [PubMed: 21964415]
47. Tan KL, Chia WC, How CW, Tor YS, Show PL, Looi QHD, et al. (2021): Benchtop Isolation and Characterisation of Small Extracellular Vesicles from Human Mesenchymal Stem Cells. *Mol Biotechnol*. 63(9):780–791. [PubMed: 34061307]
48. Chen L, Flies DB. (2013): Molecular mechanisms of T cell co-stimulation and co-inhibition. *Nat Rev Immunol*. 13(4):227–42. [PubMed: 23470321]
49. Waddell LA, Lefevre L, Bush SJ, Raper A, Young R, Lisowski ZM, et al. (2018): ADGRE1 (EMR1, F4/80) Is a Rapidly-Evolving Gene Expressed in Mammalian Monocyte-Macrophages. *Front Immunol*. 9:2246. [PubMed: 30327653]
50. Gritti D, Delvecchio G, Ferro A, Bressi C, Brambilla P (2021): Neuroinflammation in major depressive disorder: A review of PET imaging studies examining the 18-kDa translocator protein. *J Affect Disord* 292:642–651. [PubMed: 34153835]
51. Golden SA, Covington HE 3rd, Berton O, Russo SJ (2011): A standardized protocol for repeated social defeat stress in mice. *Nat Protoc* 6:1183–1191. [PubMed: 21799487]
52. Powell ND, Sloan EK, Bailey MT, Arevalo JMG, Miller GE, Chen E, et al. (2013): Social stress up-regulates inflammatory gene expression in the leukocyte transcriptome via  $\beta$ -adrenergic induction of myelopoiesis. *Proc Natl Acad Sci U S A* 110:16574–16579. [PubMed: 24062448]
53. Wohleb ES, Powell ND, Godbout JP, Sheridan JF (2013): Stress-induced recruitment of bone marrow-derived monocytes to the brain promotes anxiety-like behavior. *J Neurosci* 33:13820–13833. [PubMed: 23966702]
54. Krishnan V, Han MH, Graham DL, Berton O, Renthal W, Russo SJ, et al. (2007): Molecular adaptations underlying susceptibility and resistance to social defeat in brain reward regions. *Cell* 131:391–404. [PubMed: 17956738]
55. Kinsey SG, Bailey MT, Sheridan JF, Padgett DA, Avitsur R (2007): Repeated social defeat causes increased anxiety-like behavior and alters splenocyte function in C57BL/6 and CD-1 mice. *Brain Behav Immun* 21:458–466. [PubMed: 17178210]
56. Isingrini E, Perret L, Rainer Q, Amilhon B, Guma E, Tanti A, et al. (2016): Resilience to chronic stress is mediated by noradrenergic regulation of dopamine neurons. *Nat Neurosci* 19:560–563. [PubMed: 26878672]
57. Pertwee RG, Howlett AC, Abood ME, Alexander SPH, Marzo VD, Elphick MR, et al. (2010): International Union of Basic and Clinical Pharmacology. LXXIX. Cannabinoid receptors and their ligands: beyond CB<sub>1</sub> and CB<sub>2</sub>. *Pharmacol Rev* 62:588–631. [PubMed: 21079038]
58. Howlett AC, Barth F, Bonner TI, Cabral G, Casellas P, Devane WA, et al. (2002): International Union of Pharmacology. XXVII. Classification of cannabinoid receptors. *Pharmacol Rev* 54:161–202. [PubMed: 12037135]
59. Tam J, Vemuri VK, Liu J, Batkai S, Mukhopadhyay B, Godlewski G, et al. (2010): Peripheral CB1 cannabinoid receptor blockade improves cardiometabolic risk in mouse models of obesity. *J Clin Invest* 120:2953–2966. [PubMed: 20664173]
60. Guneykaya D, Ivanov A, Hernandez DP, Haage V, Wojtas B, Meyer N, et al. (2018): Transcriptional and translational differences of microglia from male and female brains. *Cell Rep* 24:2773–2783.e6. [PubMed: 30184509]
61. Hanamsagar R, Alter MD, Block CS, Sullivan H, Bolton JL, Bilbo SD (2017): Generation of a microglial developmental index in mice and in humans reveals a sex difference in maturation and immune reactivity. *Glia* 65:1504–1520. [PubMed: 28618077]



62. Schwarz JM, Sholar PW, Bilbo SD (2012): Sex differences in microglial colonization of the developing rat brain. *J Neurochem* 120:948–963. [PubMed: 22182318]
63. Weinhard L, Neniskyte U, Vadisiute A, di Bartolomei G, Aygun N, Riviere L, et al. (2018): Sexual dimorphism of microglia and synapses during mouse postnatal development. *Dev Neurobiol* 78:618–626. [PubMed: 29239126]
64. Pitychoutis PM, Nakamura K, Tsonis PA, Papadopoulou-Daifoti Z (2009): Neurochemical and behavioral alterations in an inflammatory model of depression: sex differences exposed. *Neuroscience* 159:1216–1232. [PubMed: 19409213]
65. Huestis MA, Cone EJ (2004): Relationship of delta 9-tetrahydrocannabinol concentrations in oral fluid and plasma after controlled administration of smoked cannabis. *J Anal Toxicol* 28:394–399. [PubMed: 15516285]
66. Cooper ZD, Haney M (2009): Comparison of subjective, pharmacokinetic, and physiological effects of marijuana smoked as joints and blunts. *Drug Alcohol Depend* 103:107–113. [PubMed: 19443132]
67. Zamberletti E, Gabaglio M, Prini P, Rubino T, Parolaro D (2015): Cortical neuroinflammation contributes to long-term cognitive dysfunctions following adolescent delta-9-tetrahydrocannabinol treatment in female rats. *Eur Neuropsychopharmacol* 25:2404–2415. [PubMed: 26499171]
68. Rubino T, Realini N, Braida D, Guidi S, Capurro V, Viganò D, et al. (2009): Changes in hippocampal morphology and neuroplasticity induced by adolescent THC treatment are associated with cognitive impairment in adulthood. *Hippocampus*. 19(8):763–72. [PubMed: 19156848]
69. Rubino T, Viganò D, Realini N, Guidali C, Braida D, Capurro V, et al. (2009): Chronic delta 9-tetrahydrocannabinol during adolescence provokes sex-dependent changes in the emotional profile in adult rats: behavioral and biochemical correlates. *Neuropsychopharmacology*. 33(11):2760–71.
70. Gabaglio M, Zamberletti E, Manenti C, Parolaro D, Rubino T. (2021): Long-Term Consequences of Adolescent Exposure to THC-Rich/CBD-Poor and CBD-Rich/THC-Poor Combinations: A Comparison with Pure THC Treatment in Female Rats. *Int J Mol Sci*. 22(16):8899. [PubMed: 34445602]
71. Lopez-Rodriguez AB, Llorente-Berzal A, Garcia-Segura LM, Viveros MP. (2014): Sex-dependent long-term effects of adolescent exposure to THC and/or MDMA on neuroinflammation and serotonergic and cannabinoid systems in rats. *Br J Pharmacol*. 171(6):1435–47. [PubMed: 24236988]
72. Konishi H, Kiyama H. (2018): Microglial TREM2/DAP12 Signaling: A Double-Edged Sword in Neural Diseases. *Front Cell Neurosci*. 12:206. [PubMed: 30127720]
73. Cabral GA, Jamerson M (2014): Marijuana use and brain immune mechanisms. *Int Rev Neurobiol* 118:199–230. [PubMed: 25175866]
74. Pasca S, Jurj A, Petrushev B, Tomuleasa C, Matei D (2020): MicroRNA-155 Implication in M1 polarization and the impact in inflammatory diseases. *Front Immunol* 11:625. [PubMed: 32351507]
75. Mahesh G, Biswas R (2019): MicroRNA-155: A master regulator of inflammation. *J Interferon Cytokine Res* 39:321–330. [PubMed: 30998423]
76. Weber MD, McKim DB, Niraula A, Witcher KG, Yin W, Sobol CG, et al. (2019): The influence of microglial elimination and repopulation on stress sensitization induced by repeated social defeat. *Biol Psychiatry* 85:667–678. [PubMed: 30527629]
77. Dhabhar FS. (2018): The short-term stress response – mother nature’s mechanism for enhancing protection and performance under conditions of threat, challenge, and opportunity. *Front Neuroendocrinol* 49:175–192. [PubMed: 29596867]
78. Dhabhar FS. (2014): Effects of stress on immune function: the good, the bad, and the beautiful. *Immunol Res* 58:193–210. [PubMed: 24798553]
79. Réu P, Khosravi A, Bernard S, Mold JE, Salehpour M, Alkass K, et al. (2017): The lifespan and turnover of microglia in the human brain. *Cell Rep* 20:779–784. [PubMed: 28746864]
80. Masuda T, Sankowski R, Staszewski O, Prinz M. (2020): Microglia Heterogeneity in the Single-Cell Era. *Cell Rep*. 30(5):1271–1281. [PubMed: 32023447]



81. Weber MD, Godbout JP, Sheridan JF. (2017): Repeated Social Defeat, Neuroinflammation, and Behavior: Monocytes Carry the Signal. *Neuropsychopharmacology*. 42(1):46–61. [PubMed: 27319971]
82. Malcangio M (2019): Role of the immune system in neuropathic pain. *Scand J Pain*. 20(1):33–37. [PubMed: 31730538]
83. Rayasam A, Fukuzaki Y, Vexler ZS. (2021): Microglia-leucocyte axis in cerebral ischaemia and inflammation in the developing brain. *Acta Physiol (Oxf)*. 233(1):e13674. [PubMed: 33991400]
84. Wagner JA, Varga K, Ellis EF, Rzigalinski BA, Martin BR, Kunos G. (1997): Activation of peripheral CB1 cannabinoid receptors in haemorrhagic shock. *Nature*. 390(6659):518–21. [PubMed: 9394002]
85. Onaivi ES, Chaudhuri G, Abaci AS, Parker M, Manier DH, Martin PR, Hubbard JR. (1999): Expression of cannabinoid receptors and their gene transcripts in human blood cells. *Prog Neuropsychopharmacol Biol Psychiatry*. 23(6):1063–77. [PubMed: 10621950]

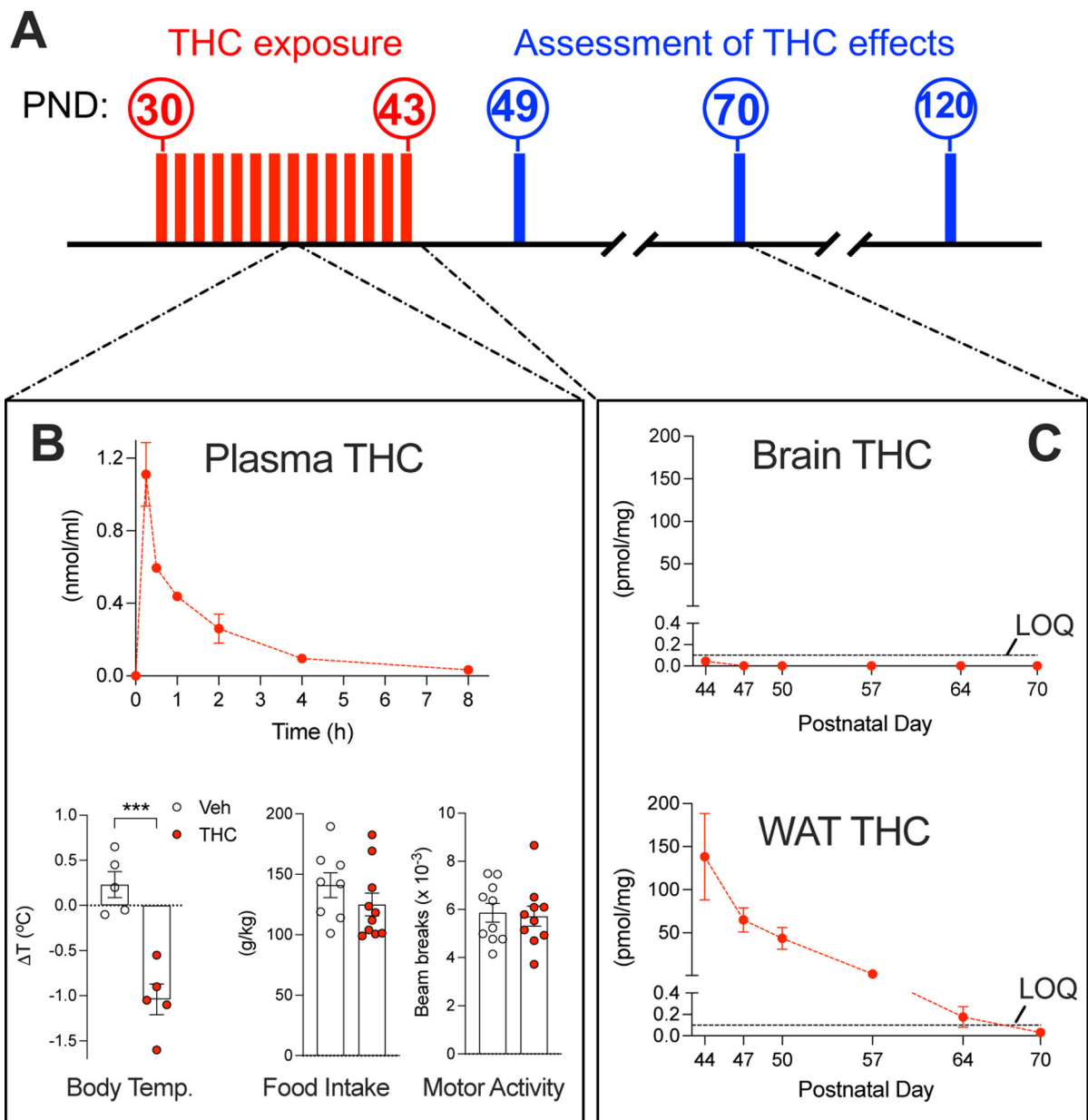


**Fig. 1. Frequent exposure to low-dose THC in adolescence: pharmacokinetic and pharmacodynamic characterization.**

(A) We modeled frequent low-level exposure to THC-containing cannabis in adolescence by administering THC (5 mg/kg, i.p.) or its vehicle (8% Tween-80 in saline, v/v) to male and female mice from PND30 to PND43. The animals were euthanized on PND49, PND70 or PND120. (B) Top: time-course of plasma THC concentrations after a single injection of THC (5 mg/kg, i.p.) to male mice on PND37 (n=5). Bottom: effects of vehicle or THC on core body temperature (30 min after injection; n = 5) (left), average daily food intake (center) and locomotor activity (right) (n=8–10). (C) Time-course of THC concentrations in brain and white adipose tissue (WAT) after THC injection (n=3–4). LOQ, lower limit of quantification. \*\*\*P < 0.001, two-tailed unpaired *t* test.

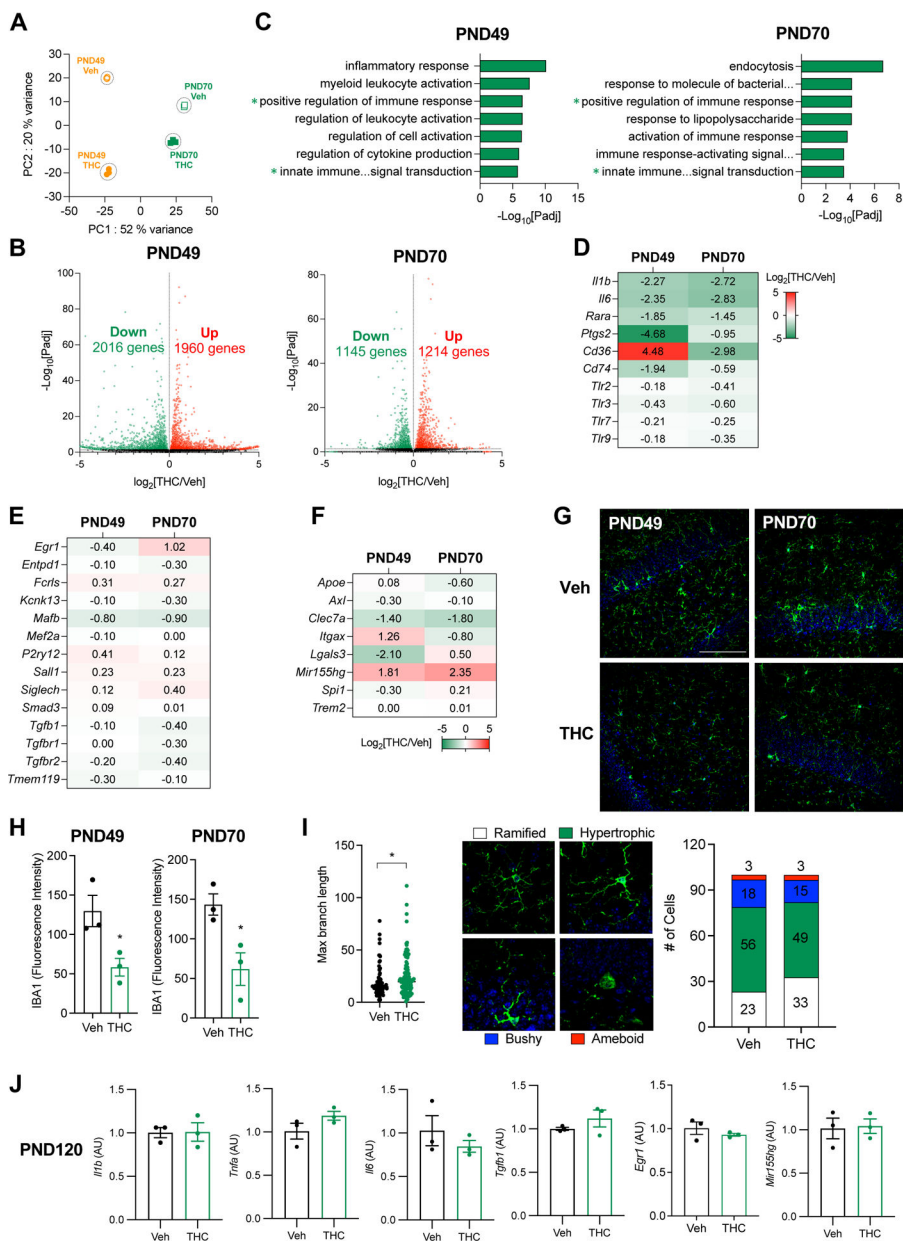


**Fig. 2. Persistent effects of adolescence THC exposure on gene transcription in microglia.** (A) Principal component analysis of RNAseq data from purified microglia of THC- and vehicle-treated male mice at PND49 and PND70 (n=3–4 per group). (B) Volcano plots showing genes that were differentially expressed (Padj<0.05) between THC- and vehicle-treated mice at PND49 and PND70. Red, transcripts upregulated in THC vs vehicle groups; green, transcripts downregulated in THC vs vehicle groups; black, unchanged transcripts (Padj>0.05). (C) Annotation of genes downregulated in THC- vs vehicle-treated mice at PND49 and PND70. Gene ontology (GO) categories showing significant enrichment in downregulated transcripts are listed according to their Padj values (lower Padj value on top). GO:0006954, inflammatory response ; GO:0002274, myeloid leukocyte activation; GO:0050778, positive regulation of immune response; GO:0002694,

regulation of leukocyte activation; GO:0050865, regulation of cell activation; GO:0001817, regulation of cytokine production; GO:0045087, innate immune response ; GO:0006897, endocytosis; GO:0002237, response to molecules of bacterial origin; GO:0032496, response to LPS; GO:0002253, activation of immune response; GO:0002757, immune response-activating signal transduction. **(D-F)** Heatmaps showing the effects of adolescence THC exposure on the transcription of select **(D)** inflammatory genes, **(E)** genes involved in microglia homeostasis, and **(F)** genes related to disease-associated microglia phenotypes. Numbers represent the  $\log_2[\text{THC}/\text{Veh}]$  value for each gene. **(G)** Confocal images of IBA-1 immunofluorescence in hippocampus of PND70 male mice after adolescence exposure to vehicle or THC. Green, IBA1; blue, DAPI. Calibration bar, 100  $\mu\text{m}$ . **(H)** Quantitative analyses of IBA1 immunoreactivity in vehicle- (black symbols) and THC-treated (green symbols) mice at PND49 and PND70. **(I)** Morphometric analysis of microglia from vehicle- and THC-treated mice at PND70. Left: maximal branch length. Middle: representative morphologies for each classification of microglia. Right: quantitative distribution (percent of total) of major microglial morphologies. **(J)** qRT-PCR analyses showing mRNA levels of select THC-sensitive genes in microglia from PND120 mice after adolescence exposure to vehicle or THC (n=3). \* $P < 0.05$ , two-tailed unpaired  $t$  test.

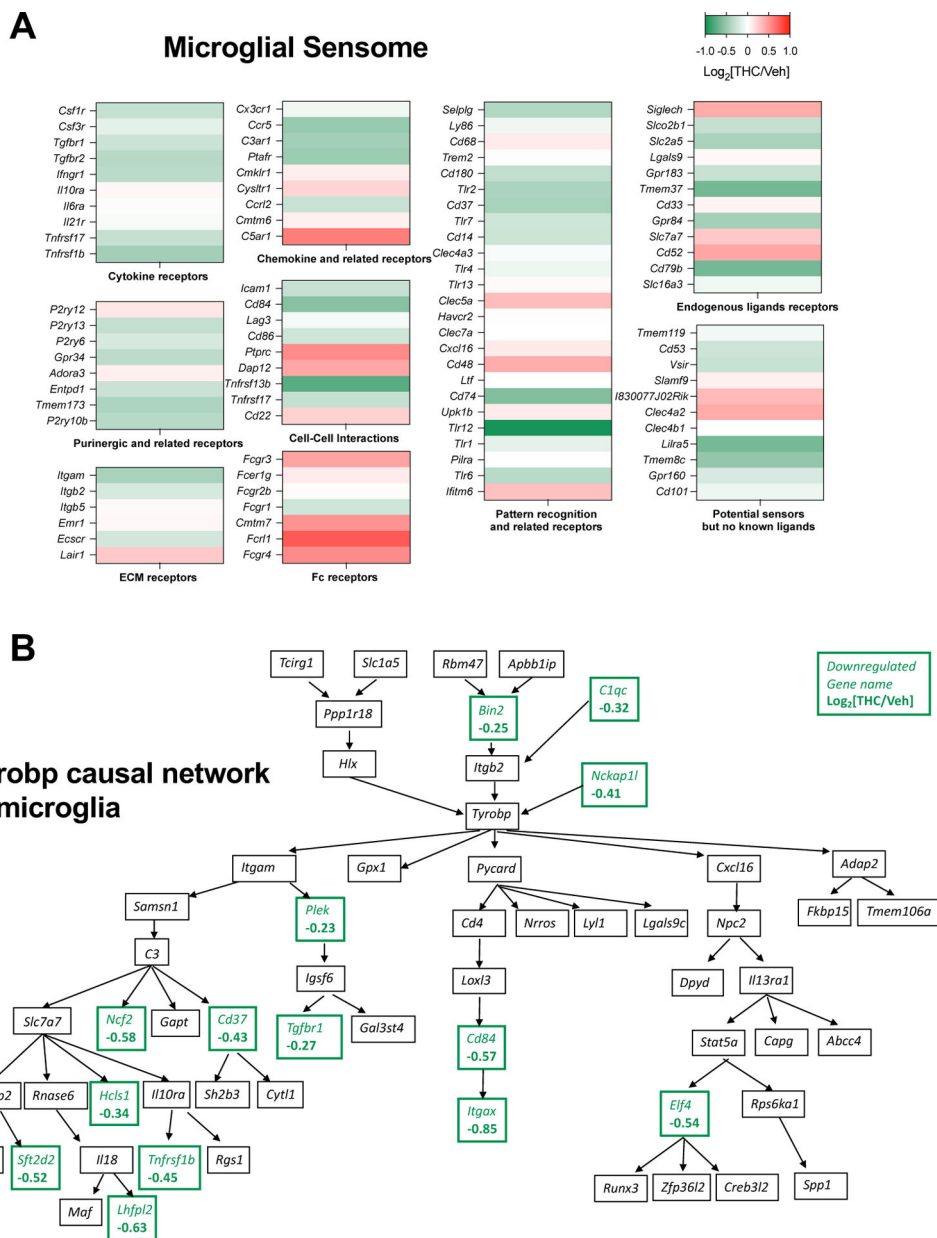


**Fig. 3. Functionally enriched networks in microglia from THC-exposed mice.** STRING multiple protein analysis of 318 down-regulated genes ( $P_{adj} < 10^{-4}$ ) in microglia of THC-treated mice identified 305 nodes and 867 edges, with PPI enrichment P-value  $< 1.0 \times 10^{-16}$ . Among the networks identified with significant enrichment by false discovery rate (FDR), two representative results are shown: **(A)** The genes of inquiry were highly enriched ( $FDR = 1.44 \times 10^{-6}$ ) in genes identified as microglial sensome (40). A heatmap showing the effects of adolescence THC exposure on the microglial sensome genes is shown. Numbers are  $\log_2[\text{THC}/\text{Veh}]$  values for each gene. **(B)** STRING also identified enrichment of the genes of inquiry in the WikiPathway WP3625, the Tyrobp causal network in microglia ( $FDR = 4.88 \times 10^{-5}$ ). The pathway WP3625 diagram is shown with the whole

network and genes affected by adolescence THC exposure in green and  $\log_2[\text{THC}/\text{Veh}]$  value for each gene.

Author Manuscript

Author Manuscript

Author Manuscript

Author Manuscript

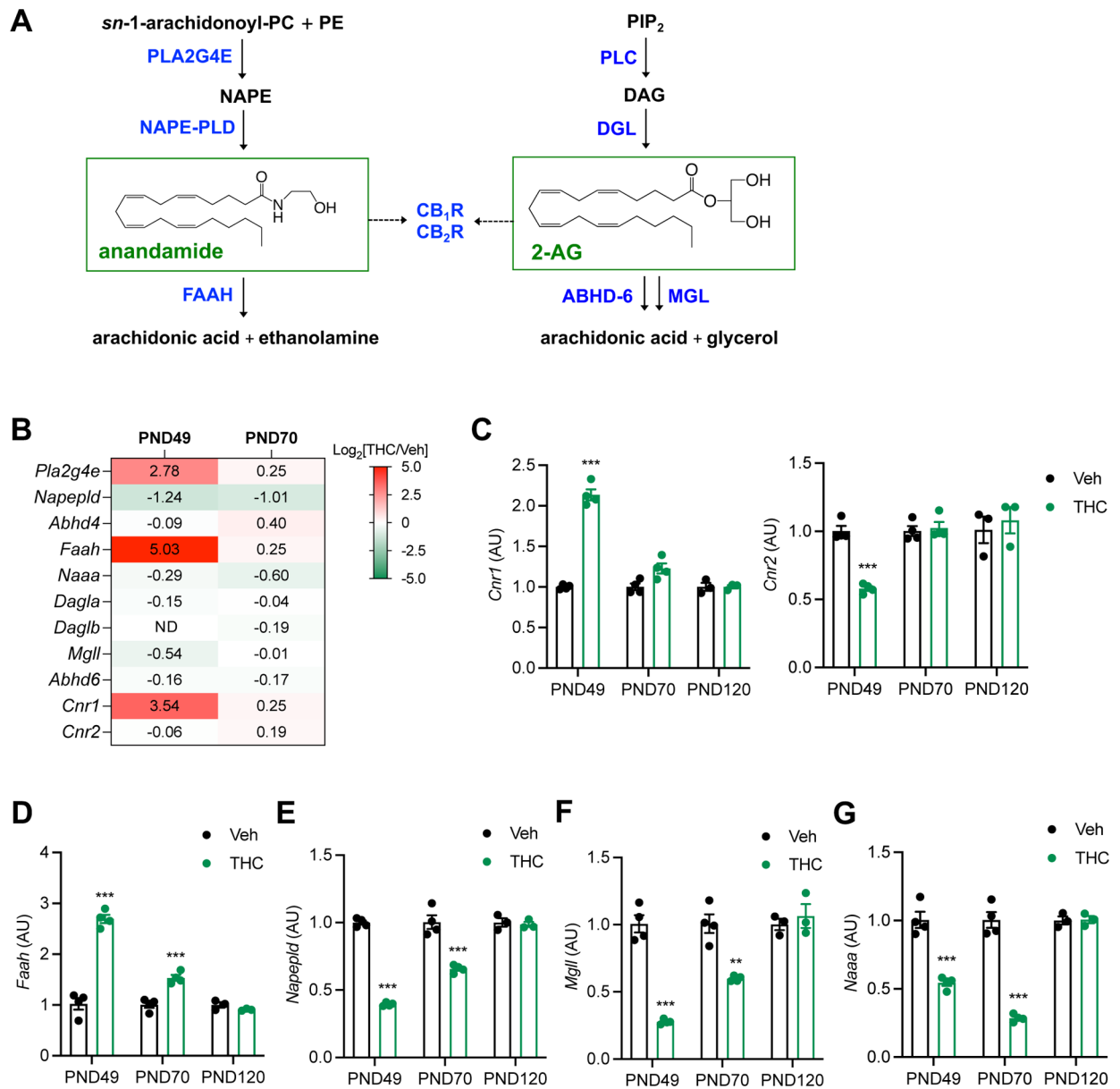


**Fig. 4. Persistent effects of adolescence THC exposure on the endocannabinoid system in microglia.**

(A) Schematic overview of the endocannabinoid signaling system. Left: anandamide formation and deactivation. Right, 2-arachidonoyl-*sn*-glycerol (2-AG) formation and deactivation. Abbreviations: PC, phosphatidylcholine; PE, phosphatidylethanolamine; PLA2G4E, phospholipase A<sub>2</sub> group IVE; NAPE, N-acyl-PE; NAPE-PLD, NAPE-specific phospholipase D; FAAH, fatty acid amide hydrolase; PIP<sub>2</sub>, phosphatidylinositol-4,5-bisphosphate; PLC, phospholipase C; DAG, diacylglycerol; DGL, diacylglycerol lipase; ABHD-6,  $\alpha$ , $\beta$ -hydrolase domain-containing 6; MGL, monoglyceride lipase. (B-G) Changes in the levels of primary endocannabinoid-related genes produced in microglia by adolescence exposure to THC. (B) Bulk RNAseq analysis of purified microglia (n=3-4). (C-G) qRT-PCR quantification (normalized to individual vehicle controls) of transcripts



encoding (C) CB<sub>1</sub> (*Cnr1*) and CB<sub>2</sub> (*Cnr2*) receptors; (D) FAAH (*Faah*); (E) NAPE-PLD (*Napepld*); (F) MGL (*Mgl1*) and (G) N-acylethanolamine acid amidase (*Naaa*) (n=3). \*\*P < 0.01 and \*\*\*P < 0.001, two-tailed unpaired *t* test.

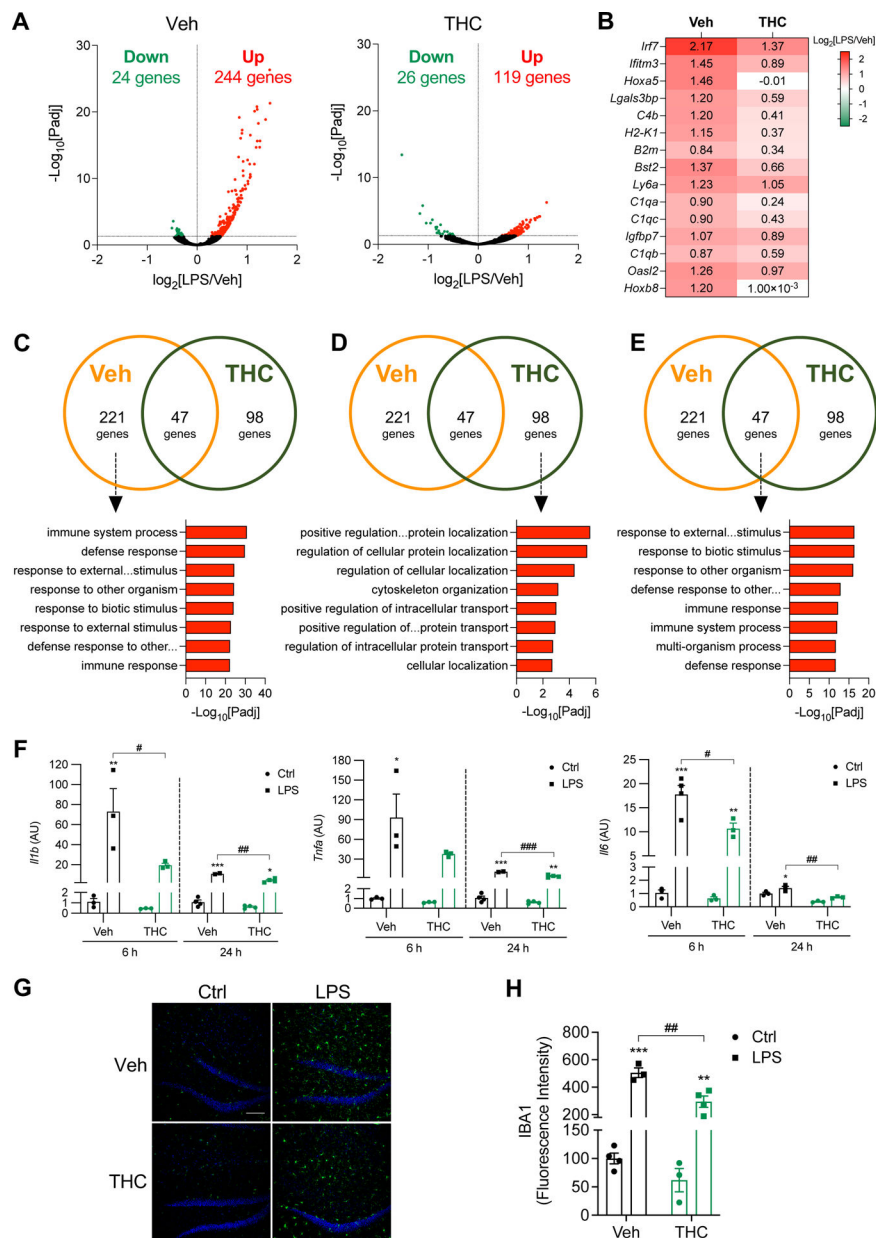


**Fig. 5. Persistent effects of adolescence THC exposure on the response to LPS.** (A) Volcano plots showing genes differentially expressed (Padj<0.05) in brain tissue between THC- and vehicle-treated male mice 24h after LPS challenge (0.33 mg/kg, i.p., challenge on PND70). Left, vehicle; right, THC. Red, transcripts upregulated by LPS; green, transcripts downregulated by LPS; black, unchanged transcripts (Padj>0.05). (B) Heatmap showing changes elicited by LPS on the transcription of select innate immune genes. Numbers represent log<sub>2</sub>[LPS/Veh] values. (C-E) Gene Ontology (GO) analyses illustrating the differential impact of LPS in brain tissue from THC- and vehicle-treated mice. Number of genes and GO categories enriched in: (C) only the vehicle group, (D) only the THC group, and (E) both vehicle and THC groups. GO categories are listed according to their Padj values (lower Padj value on top). GO:0002376, immune

system process; GO:0006952, defense response; GO:0043207, response to external biotic stimulus; GO:0051707, response to other organism; GO:0009607, response to biotic stimulus; GO:0009605, response to external stimulus; GO:0098542, defense response to other organism; GO:0006955, immune response; GO:1903829, positive regulation of cellular protein localization; GO:1903827, regulation of cellular protein localization; GO:0060341, regulation of cellular localization; GO:0007010, cytoskeleton organization; GO:0032388, positive regulation of intracellular transport; GO:0090316, positive regulation of intracellular protein transport; GO:0033157, regulation of intracellular protein transport; GO:0051641, cellular localization; GO:0051704, multi-organism process. **(F)** Transcription of representative cytokines (*Il1b*, *Tnfa* and *Il6*) in brain tissue after LPS in THC- or vehicle-treated mice (n=3 per group). **(G)** Confocal images of IBA-1 immunofluorescence in hippocampus of THC- or vehicle-treated mice 24h after LPS. Green, IBA1; blue, DAPI. Calibration bar, 100  $\mu$ m. **(H)** Quantitative analyses of IBA1 immunoreactivity in vehicle- and THC-treated mice that received LPS or saline. \*/#P < 0.05, \*\*/##P < 0.01, and \*\*\*/###P < 0.001, two-way ANOVA, followed by Tukey's multiple comparison test.

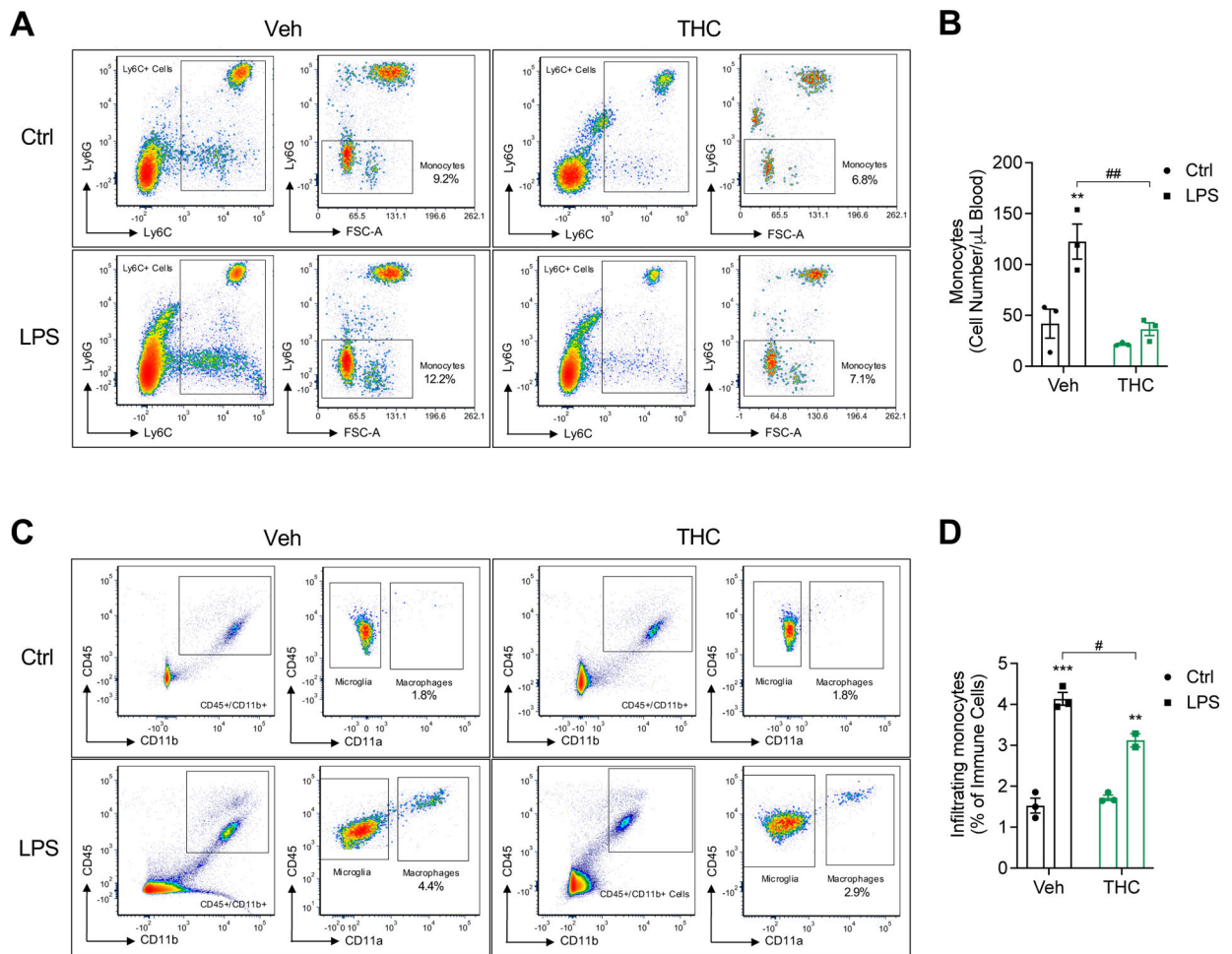


**Fig. 6. Persistent effects of adolescence THC exposure on LPS-induced monocyte trafficking.** (A) Gating strategy for the isolation of circulating Ly6C<sup>+</sup>Ly6G<sup>-</sup> monocytes, and (B) number of monocytes in vehicle- and THC-treated male mice challenged with LPS or saline (Ctrl). Data are expressed as number of cells per  $\mu$ L of blood. (C) Gating strategy for the isolation of CD45<sup>+</sup>CD11b<sup>+</sup>CD11a<sup>+</sup> monocytes trafficking to brain tissue, and (D) number of infiltrating monocytes in vehicle- and THC-treated male mice challenged with LPS or saline. Expression of CD11a was used to distinguish infiltrating monocytes (CD11a<sup>hi</sup>) from microglia (CD45<sup>+</sup>CD11b<sup>+</sup>CD11a<sup>lo</sup>). # $P < 0.05$ , \*\*/# $P < 0.01$ , and \*\*\* $P < 0.001$ , two-way ANOVA followed by Tukey's multiple comparison test.

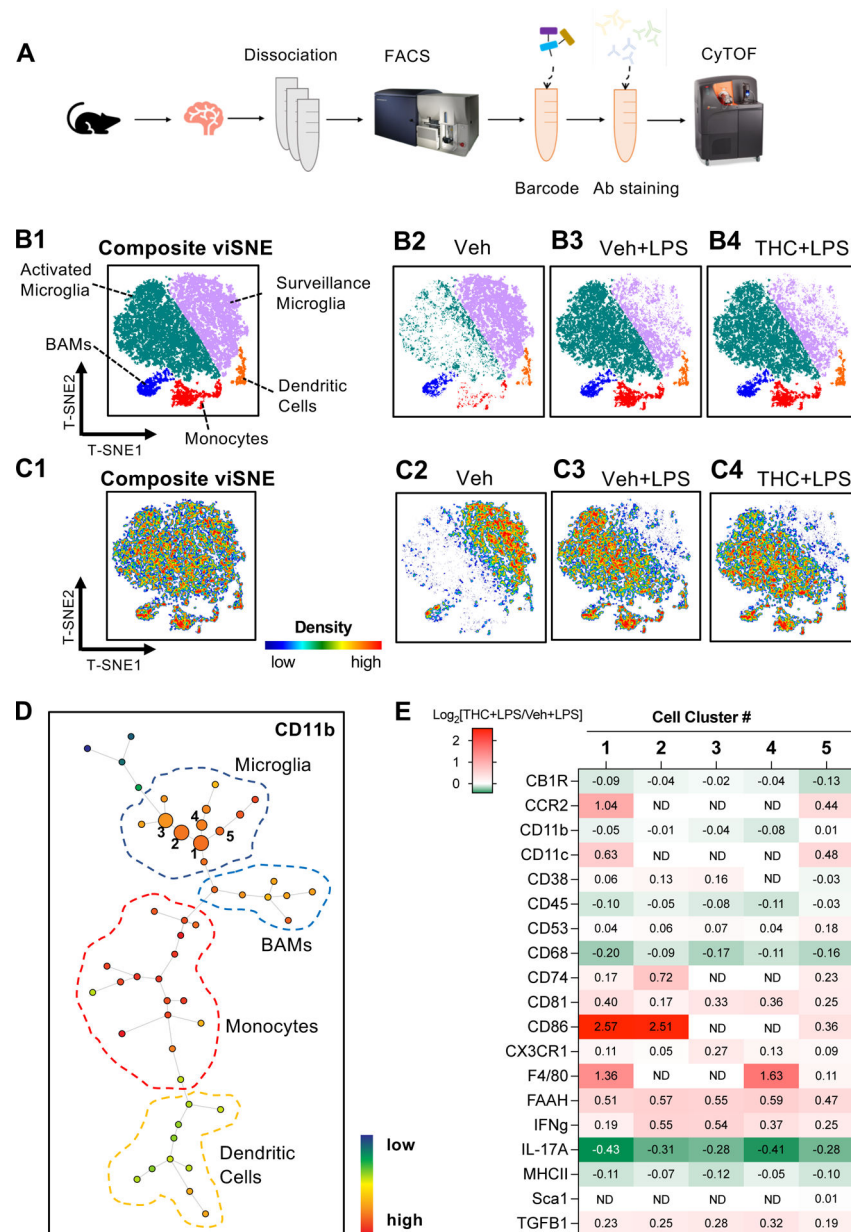


**Fig. 7. CyTOF analysis of immune cells from the brain of adult mice after adolescence THC exposure.**

(A) Schematics illustrating the cyTOF protocol. (B) ViSNE plots for composite (B1) and for each experimental group (B2-B4), color-coded for five (sub)population of brain immune cells: surveillant and activated microglia, border-associated macrophages (BAMS), monocytes, and dendritic cells. (C) ViSNE plots with cell density heatmap, for composite (C1) and for each experimental group (C2-C4). (D) SPADE diagram for CD11b in brain immune cells, which identifies five microglia cell clusters that differ between control and THC-treated mice. (E) Heatmap showing differences in marker protein expression in each microglia cell cluster. Numbers are the  $\log_2[\text{THC}/\text{Veh}]$  values for each marker.

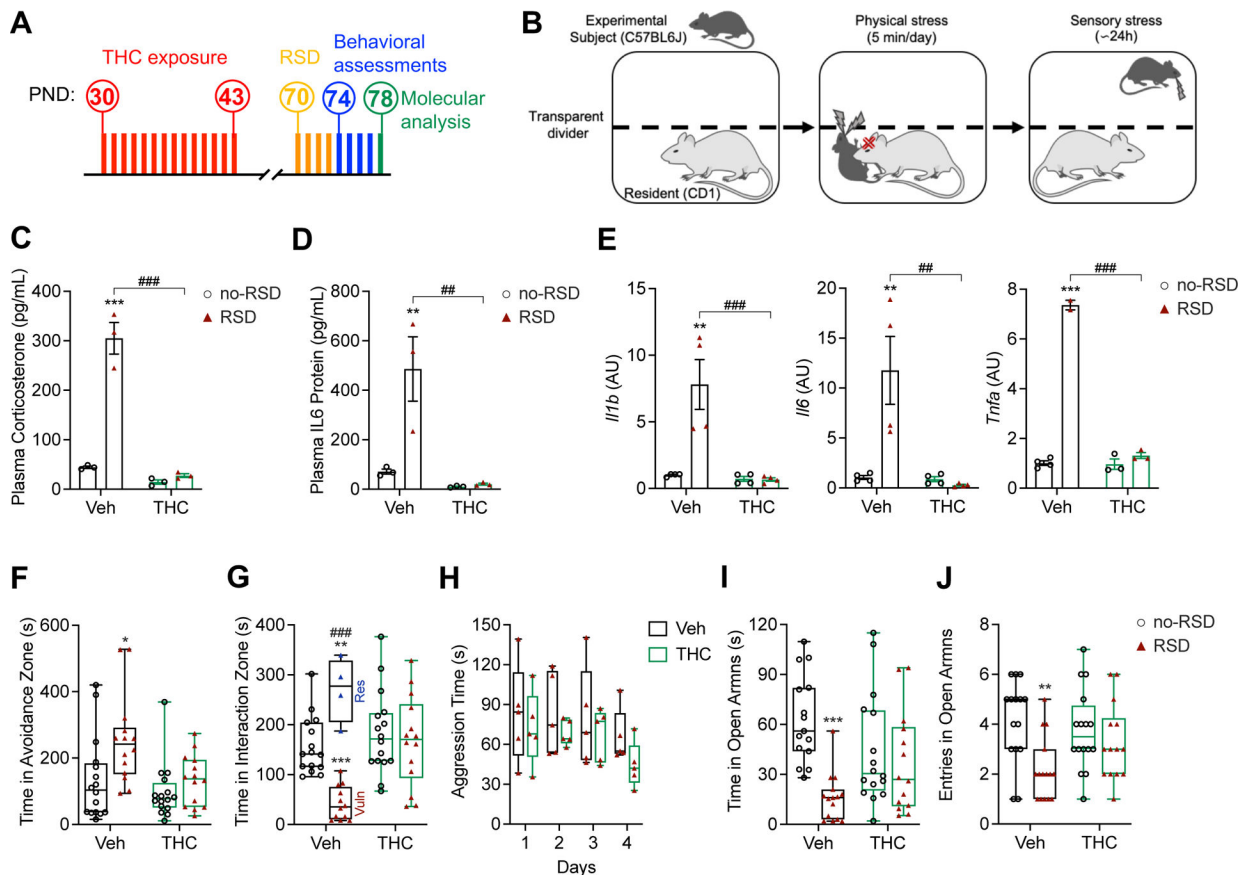


**Fig. 8. Persistent effects of adolescence THC exposure on repeated social defeat (RSD)-induced molecular and behavioral deficits in mice.**

(A, B) Schematics illustrating the THC administration and testing protocols. Plasma levels of (C) corticosterone and (D) IL-6 protein in vehicle- or THC-treated male mice 24h after RSD ( $n=3$  per group). (E) Levels of *Il1b*, *Il6* and *Tnfa* mRNA in brain tissue 24h after RSD ( $n=3$  per group). (F, G) Effects of RSD in the social interaction test. (F) Time spent in the avoidance zone (s). Vehicle-treated mice showed a significant preference for the avoidance area ( $F_{1, 56} = 7.894$ ,  $P = 0.0068$ ). (G) Distribution of time spent in the interaction zone (s). Vehicle-treated mice did not distribute normally ( $A^{2*} = 1.331$ ;  $P = 0.0012$ ) and a k-means analysis uncovered two sub-groups of ‘vulnerable’ [Vuln, red closed circles; ~75% ( $n=12$ )] and ‘resilient’ mice [Res, blue closed circles; ~25% ( $n=4$ )]. Vulnerable animals avoided, whereas resilient preferred the interaction zone ( $F_{1, 56} = 7.894$ ,  $P = 0.0068$ ). RSD did not significantly affect social behavior in THC-treated mice ( $n=14-16$ ). (H) Aggression time (s) in vehicle- and THC-treated mice ( $F_{1, 32} = 2.845$ ,  $P = 0.1014$ ). (I, J) Effects of RSD in the EPM test. (I) Time in open arms. (J) Number of open arm entries. RSD did not significantly affect anxiety-like behavior in THC-treated mice ( $n=14-16$ ).  $*/\#P < 0.05$ ,  $*/\#\#P < 0.01$ , and  $*/\#\#\#P < 0.001$ , two-way ANOVA followed by Tukey’s multiple comparison test.

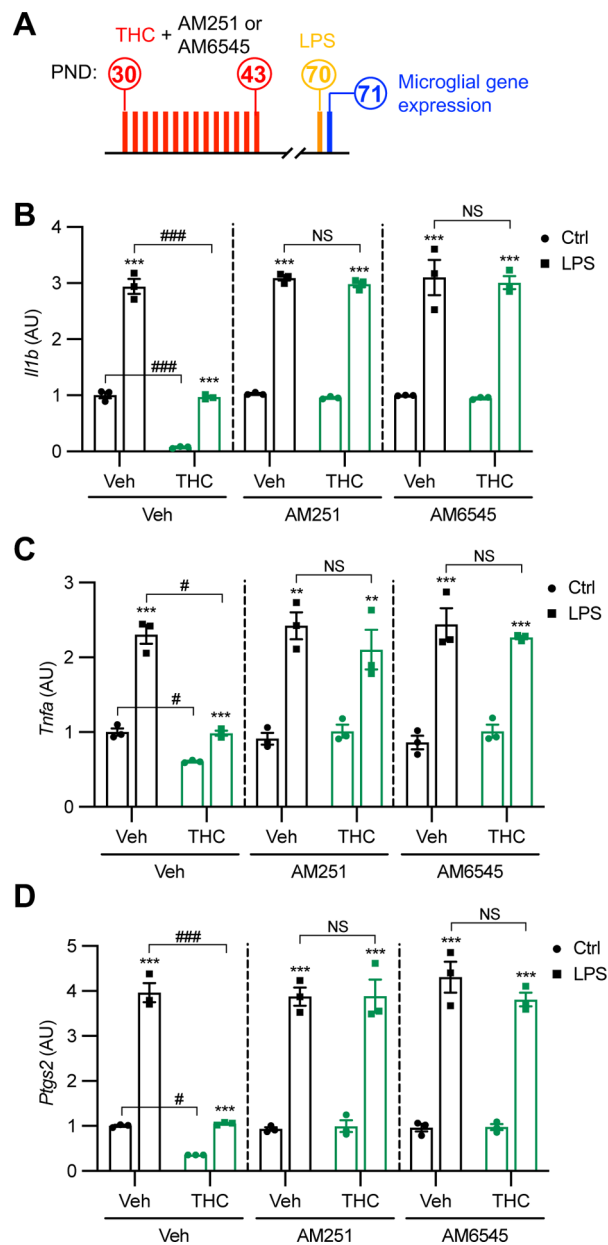


**Fig. 9. The effects of adolescence THC exposure in microglia require peripheral CB<sub>1</sub> receptors.** (A) Schematics illustrating the THC administration and testing protocols. Gene expression in purified microglia was measured by qRT-PCR (n=3 per group). Levels of (B) *I11b*, (C) *Tnfa*, and (D) *Ptgs2* in male mice treated with vehicle or THC alone (left), vehicle or THC plus the globally active CB<sub>1</sub> inverse agonist AM251 (1 mg/kg, i.p.) (center) and vehicle or THC plus the peripherally restricted CB<sub>1</sub> neutral antagonist AM6545 (3 mg/kg, i.p.). #P < 0.05, \*\*P < 0.01, and \*\*\*/###P < 0.001, two-way ANOVA followed by Tukey's multiple comparison test.



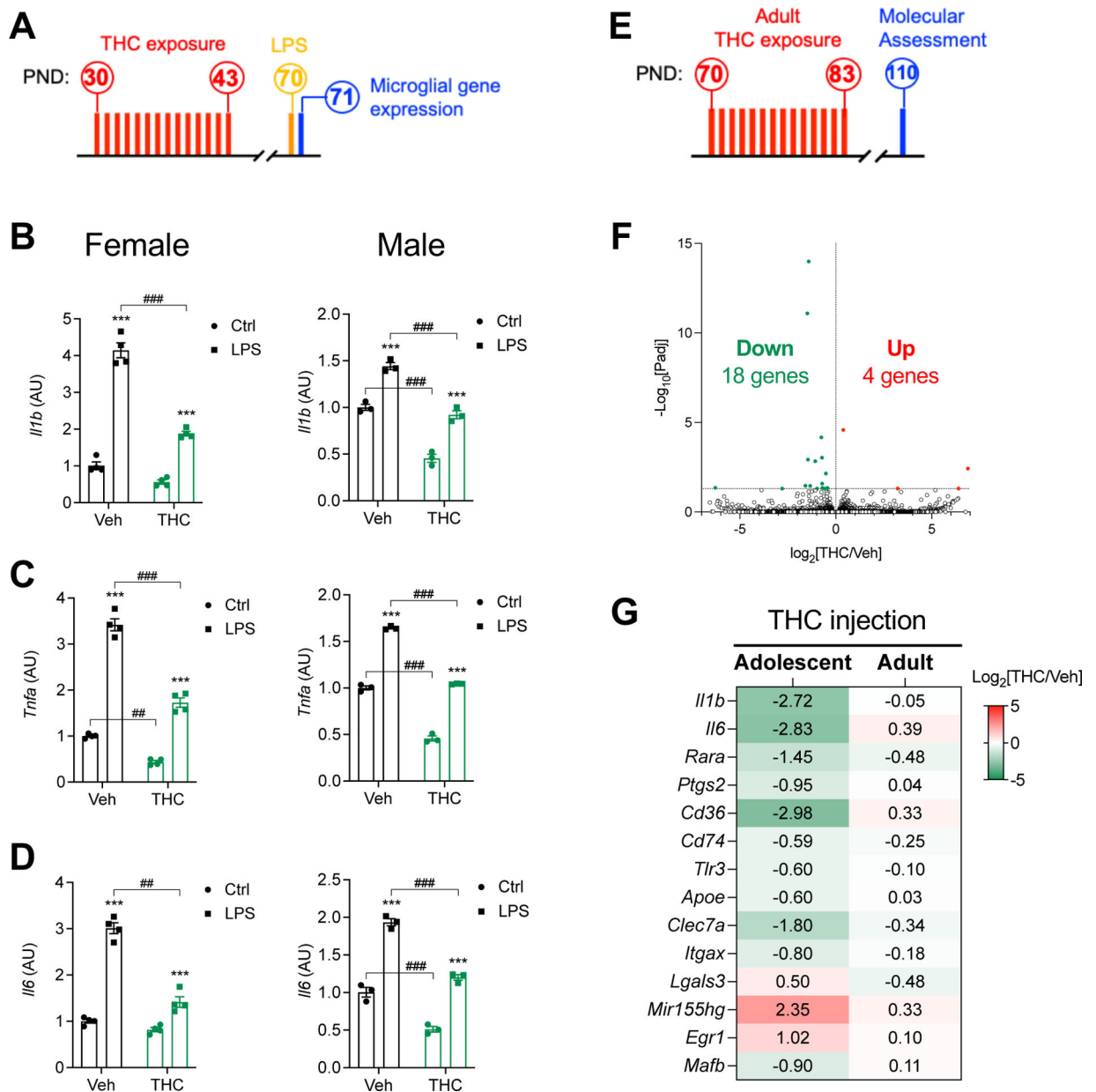


**Fig. 10. The effects of adolescence THC exposure on microglia are sexually dimorphic and age-dependent.**

(A) Schematics illustrating the THC administration and LPS challenge protocols used in adolescent female mice. Gene expression in microglia was measured by qRT-PCR ( $n=3$  per group). Levels of (B) *Il1b*, (C) *Tnfa* and (D) *Il6* mRNA in female (left) and male (right) mice exposed to vehicle or THC and then challenged with LPS. (E) Schematics illustrating the THC administration protocol used in adult male mice. The animals received daily vehicle or THC injections (5 mg/kg, i.p.) from PND70 to PND83. Gene expression in microglia was assessed by bulk RNA-seq on PND110. (F) Volcano plots showing genes that were differentially expressed ( $Padj < 0.05$ ) between THC and vehicle groups at PND110. Red, transcripts upregulated in THC vs vehicle; green, transcripts downregulated in THC vs vehicle; black, unchanged transcripts ( $Padj > 0.05$ ). (G) Heatmap comparing the effects of

adolescence vs adult treatment with THC. Numbers represents the  $\log_2[\text{THC}/\text{Veh}]$  value for each gene. ##P < 0.01 and \*\*\*/###P < 0.001, two-way ANOVA followed by Tukey's multiple comparison test.

Author Manuscript

Author Manuscript

Author Manuscript

Author Manuscript